Landsat Coverage of the Earth at High Latitudes

Robert Bindschadler

Abstract

Overlapping coverage of Landsat imagery at high latitudes is examined systematically and quantitatively. The Earth is separated into "row strips" aligned with the Landsat World Reference System (WRS), and the multi-scene coverage of Landsat imagery is divided into three types of areas: extended, missing, and overlap. Varying image orientation and narrowing row-strip width with increasing latitude are shown to have major impacts on these three areas. The dependencies of these coverage areas on skipping image collections from adjacent paths are calculated. This forms the basis for sampling strategies that can significantly reduce the number of images required to obtain full ground coverage at high latitudes. The calculations show that Antarctica can be covered with approximately one-third the total number of scene opportunities.

Introduction

Optical imagers onboard the Landsat series of satellites have been collecting data of the Earth's surface for nearly 30 years. Nowhere have these data been more valuable as a means to measure change than in the polar regions, where remoteness and harsh environments severely limit the ability to obtain long-term observational records.

Satellite observations at high latitudes have a "feast-or-famine" character. On the one hand, the spacing between satellite orbits decreases at high latitudes, increasing the density of coverage relative to low and mid-latitudes. However, for instruments whose measurement swath does not reach the geographic pole when the satellite is at its highest latitude, a data void is created centered at the pole.

Landsat data have this bi-modal character. Nothing can be done to fill the data void with an instrument that does not image that area, yet in the surrounding area, the coverage is more extensive than anywhere else on the Earth. This has provided researchers who wish to obtain data for high-latitude targets more frequent opportunities than the 16-day repeat cycle of the satellite. In the new system of Landsat operations, wherein data are collected in accordance with a standing set of image requests (Arvidson *et al.*, 2001), instrument resources should not be overspent in the polar regions by oversampling a relatively slowly changing portion of the Earth. The present Landsat strategy identifies redundant requested scenes at high latitudes based on the reduced longitudinal spacing between successfully acquired scenes (Gasch, personal communication, 2001).

This report examines the peculiar spatial sampling by Landsat instruments of the high latitudes and presents calculations of the multiple-scene coverage that can guide strategies of spatial sampling. A similar approach can be adopted to investigate coverage redundancies of other near-polar orbiting imagers.

The World Reference System

The World Reference System (WRS) refers to the regular grid of locations on the Earth at which scenes from Landsat instruments are centered (Landsat 7 Science Data Users Handbook, Chapter 5-Orbit & Coverage, URL: http://ltpwww.gsfc.nasa.gov/IAS/handbook/handbook_htmls/chapter5/chapter5.html, last accessed 06 August 2003). Landsats 1, 2, and 3 carried a series of Multi spectral Scanners (MSS) along the original WRS. A slight change in orbit period for subsequent Landsats (4, 5, and 7), carrying MSSs, Thematic Mappers (TM), and Enhanced Thematic Mapper Plus (ETM+) resulted in a modified WRS, called the WRS-2. In this report, the WRS-2 is used.

Landsats have always operated in sun-synchronous orbits. Landsat 7 crosses the equator from north to south on a descending orbital node at approximately 10:00 AM on each pass. Each orbit takes nearly 99 minutes, and the spacecraft completes just over 14.5 orbits per day, covering the entire Earth between 81.8° north and south latitude every 16 days. Figure 1 shows the pattern of descending orbits.

The Landsat 7 orbit repeats after exactly 233 orbits over exactly 16 days. The along-track segmentation of image data subdivides each orbit into exactly 248 segments. Thus, the WRS-2 indexes orbits (paths) and latitude positions (rows) into a global grid system comprising 233 paths by 248 rows. Row number increases sequentially in time, with row 60 coinciding with the equator (descending node). Row 122 is the southernmost row, rows 123 to 245 comprise the ascending portion of the orbit, row 246 is the northernmost row, and rows 247 and 248 begin the descending portion of the next orbit (path) leading smoothly to row 1.

Paths are numbered sequentially in longitude, increasing to the west. Temporal ordering of paths is not continuous. The path immediately west of a specific path, although only one path number greater, is traveled one week later. The path immediately east is traveled nine days later. WRS path/row maps are available from the EROS Data Center and have the original WRS used for Landsats 1, 2, and 3 on one side and the WRS-2 used for Landsats 4, 5, and 7 on the reverse side.

Engineering capabilities and scientific requirements dictated the initial form of the Landsat orbit, while organizational simplicity drove the formation of the WRS systems. This grid system has persevered as a system familiar to those who

Code 971, NASA Goddard Space Flight Center, Greenbelt, MD 20771 (Robert.A.Bindschadler@nasa.gov).

Photogrammetric Engineering & Remote Sensing
Vol. 69, No. 12, December 2003, pp. 1333–1339.

0099-1112/03/6912–1333$3.00/0

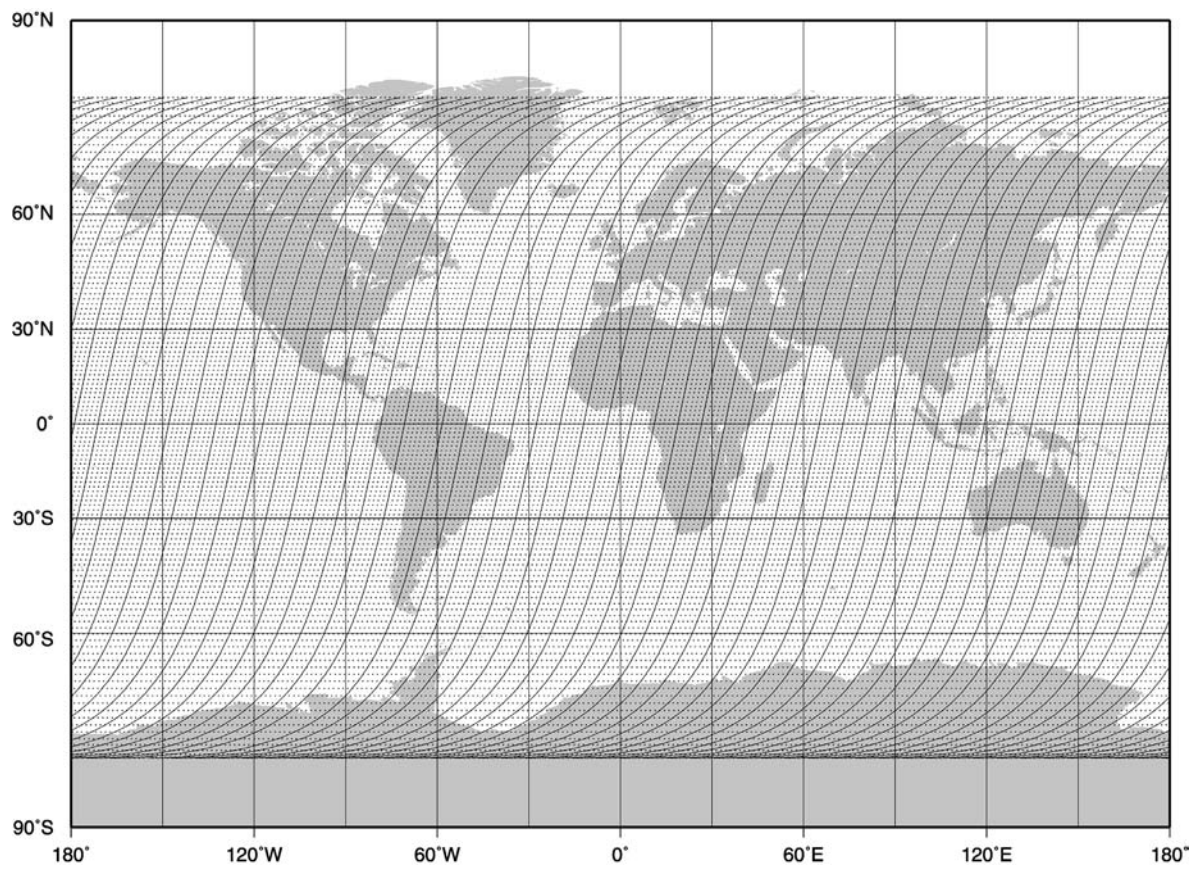

Figure 1. WRS-2 groundtrack map of descending paths and rows. Dots indicate scene centers. Solid line every fifth path.

seek to combine new and old Landsat data. It will likely continue into the future.

Local time along the Landsat groundtrack varies slowly at low and mid-latitudes, but more rapidly at higher latitudes as plotted in Figure 2. Because the satellite travels east to west across longitudes at a rate faster than the rotation of the Earth, local time along the groundtrack runs backward. Thus, local times on descending orbits in the Northern Hemisphere are later than the 10:00 AM equator crossing, while in the Southern Hemisphere local times on descending orbits are earlier than 10:00 AM. Most of these descending orbit segments occur during daylight.

Local time continues to run backward along ascending orbit segments with the northward equator crossing occurring at about 10:00 PM. Ascending orbit segments are traveled generally in darkness. Exceptions occur at the high latitudes, where extended daylight during polar summers afford the opportunity for imaging of the sunlit surface on ascending orbit segments.

The ETM+ sensor onboard Landsat 7 obtains data along the ground track at a fixed width of approximately 185 km. Westward motion of the sensor relative to the Earth during imaging causes the image to be slightly skewed relative to the orientation of the groundtrack. Images along track are produced every 23.92 seconds along-track, roughly 170 km, to produce nearly square images.

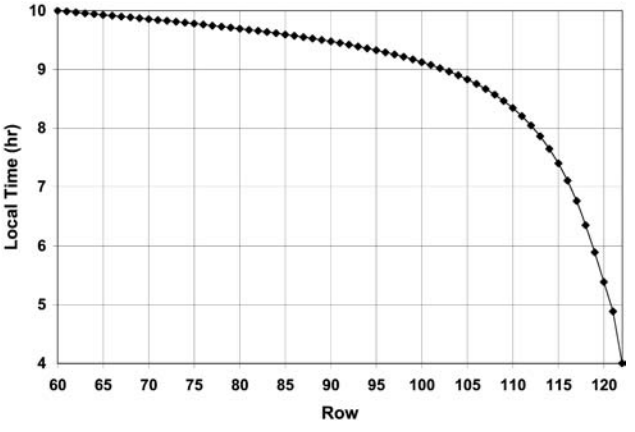

Figure 2. Local time along descending path versus WRS-2 row. Only the Southern Hemisphere portion of the descending orbit segment is shown. For the descending orbit segment in the Northern Hemisphere, the local times are progressively later with decreasing row to a maximum of 4:00 PM at row 246 (three rows north of row 1).

Multiple-Scene Coverage

Geometry

It has always been a Landsat mission requirement to provide complete coverage of the Earth (with the exception of the inevitable data voids at the poles). This is accomplished incrementally by the accumulated coverage of discrete images. The instrument's field of view dictates the image width, the parsing of the data stream along track dictates the image length, and the orbit geometry dictates the orientation of the image. This geometry is independent of path, but, as discussed below, highly dependent on row.

The coverage of areas larger than a single image scene is examined by applying the geometry illustrated in Figure 3. As mentioned earlier, each Landsat scene is roughly 170 km in along-track length (D) and 185 km in cross-track width (E). This rectangular assumption ignores the skewness of the sides of the image discussed earlier. Skewness makes images parallelepipeds rather than rectangles; however, skewness is never severe. At higher latitudes the decreased rate of motion of the Earth's surface more than offsets the increasing bearing of satellite motion, so skewness decreases at high latitudes where the issues of overlapping coverage and path skipping are prevalent. At low latitudes, the more rectilinear geometry of adjacent scenes results in the skewed sides of adjacent scenes overlapping very much like the sides of the rectangular shape assumed here. Thus, neglecting skewness causes negligible errors in this analysis.

The origin of the rectilinear system is centered on a scene and is oriented parallel to latitude (x-axis) and longitude (y-axis). The angular orientation of the scene, ϕ, corresponds to the bearing (clockwise from North) of the groundtrack and is a function of the scene-center latitude, θ.

Figure 4 shows how these two parameters vary along the southern portion of the descending orbit. The latitude of the scene centers progresses at a relatively steady rate until the most southerly latitudes. It changes very slowly near the southern extreme because the satellite is traveling across meridians of longitude very rapidly as it ends the descending portion of its orbit. This rapid cross-longitude velocity is also evident in the rapid variation of local time at high latitudes (c.f., Figure 2). On the other hand, groundtrack bearing begins to change at mid-latitudes and increases ever faster at high latitudes. Bearing changes earlier than latitude because bearing changes are influenced by the decreasing distance between meridians of longitude at higher latitudes.

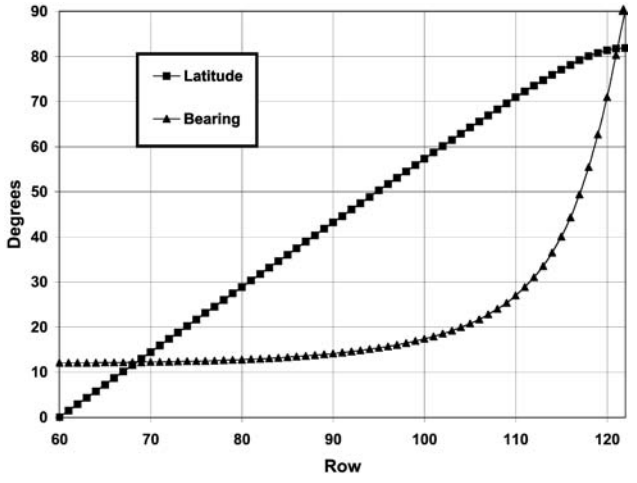

Figure 4. Scene-center latitude and groundtrack bearing (clockwise from true South, for plotting simplicity) versus WRS-2 rows 60 to 122 (the Southern Hemisphere portion of the descending orbit segment).

Row Strip

The next step in this analysis introduces the concept of a "row strip." This is the interval of latitude centered on a particular WRS-2 row. Its length equals the full circumference of the Earth along that parallel of latitude and its width is one-half of the distance between the centers of rows above and below the row being considered.

The width of the row strips is shown in Figure 5. It is directly related to the slope of the latitude curve in Figure 4. It is equal to 160 km at the equator due to the angle of the 170-km-long scene. A minimum value of 14 km is calculated

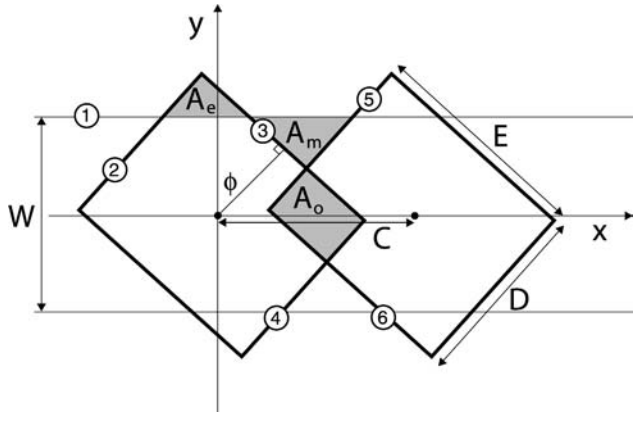

Figure 3. Geometry of overlapping Landsat scenes (heavy outlines). X-axis is latitude parallel and y-axis is longitude parallel. Image dimensions are D = 170 km and E = 185 km. Circled numbers indicate lines used in calculations. Other parameters are explained in text.

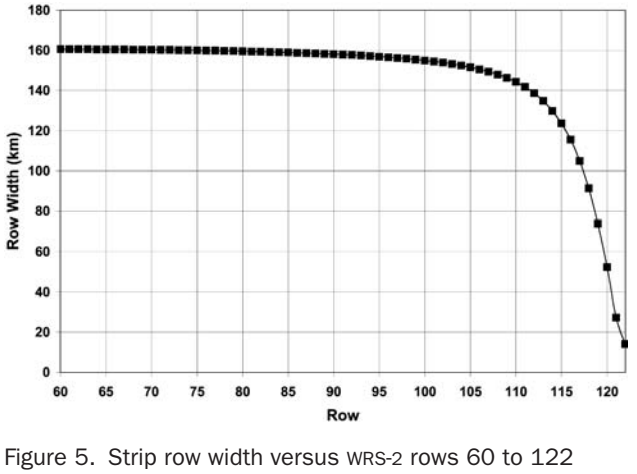

Figure 5. Strip row width versus WRS-2 rows 60 to 122 (the Southern Hemisphere portion of the descending orbit segment).

at row 122 by doubling the distance between the center latitudes of rows 121 and 122.

The introduction of row strips allows multiple-scene coverage to be addressed by calculating how effectively the row strip is covered by the scenes along that row, as scene inclination angle and number of scenes change. This concept is added to the geometry of Figure 3 by indicating the row strip by a latitude band of width W centered on the scene center.

Extended Coverage

Due to the non-zero bearing of the orbit groundtrack, part of each scene centered on a particular row extends beyond the corresponding row strip. Here this area is referred to as "extended coverage" and is denoted A_e. The equations are presented below for calculating A_e. All areas are calculated to be the total area on both sides of the row center.

Multiple Scenes

Much of the coverage issue depends on the combined coverage of adjacent scenes. The approach here focuses on the ability of scenes on the same row, but different paths, to cover the area of that row strip. Figure 3 introduces a second scene adjacent to the first. This scene is on the same row; thus, it has the same latitude and bearing, but the scene centers are separated by a distance C. Because the effects of skipping some number of adjacent paths will be examined, this distance will be generalized to $N*C$, where N is the number of paths to the next scene and C is the distance to the adjacent path.

Missing Coverage

The introduction of a second scene illustrates the formation of a second key area. Because the scenes are separated and inclined to the latitude axis, there is the possibility of some of the row strip not being included in either scene. Here this area is referred to as the "missing coverage" because it lies within the row strip, yet the scenes along this row have failed to cover it. It is denoted A_m.

Overlap Coverage

The third area is the "overlap coverage," A_o, shared between the two scenes. It lies primarily within the row strip but, in cases of large overlap, some of A_o might extend outside the row strip and duplicate A_e.

Equations

The formulas for calculating the areas of the above coverages follow directly from the geometry of Figure 3. Six lines are indicated in the figure by circled numbers. The equations of these six lines are

$$\text{Line 1: } y = \tfrac{1}{2}W \tag{1}$$

$$\text{Line 2: } y = x \tan\phi + E/(2\cos\phi) \tag{2}$$

$$\text{Line 3: } y = x \cot\phi + D/(2\sin\phi) \tag{3}$$

$$\text{Line 4: } y = x \tan\phi - E/(2\cos\phi) \tag{4}$$

$$\text{Line 5: } y = (x - N*C)\tan\phi + E/(2\cos\phi) \tag{5}$$

$$\text{Line 6: } y = (N*C - x)\cot\phi - D/(2\sin\phi) \tag{6}$$

The boundary between consecutive along-track scenes is line 3. It must intersect the groundtrack between these scenes at the midpoint. Line 1, the row strip boundary, must also intersect this midpoint. Therefore,

$$W = D\sin\phi. \tag{7}$$

The calculation of areas depends on the determination of intersection points of various pairs of the above lines. These are denoted X_{ab} for the x-value of the intersection of lines a and b. Using this notation,

$$X_{13} = (D\cos\phi)/2 \tag{8}$$

and

$$X_{12} = (D\sin\phi\cos\phi - E)/(2\sin\phi). \tag{9}$$

The distance between these two points gives the length of the hypotenuse of a right triangle with internal angle ϕ. Thus, the area of two of these triangles is

$$A_e = (X_{13} - X_{12})^2 \cos\phi\sin\phi = E^2/(4\tan\phi). \tag{10}$$

Similarly,

$$X_{15} = N*C + (D\sin\phi\cos\phi - E)/(2\sin\phi) \tag{11}$$

so that

$$\begin{aligned} A_m &= (X_{15} - X_{13})^2 \cos\phi\sin\phi \\ &= [N*C - E/(2\sin\phi)]^2 \cos\phi\sin\phi. \end{aligned} \tag{12}$$

Finally,

$$X_{35} = \tfrac{1}{2}(D\cos\phi - E\sin\phi) + N*C\sin^2\phi, \tag{13}$$

$$X_{34} = \tfrac{1}{2}(D\cos\phi + E\sin\phi), \text{ and} \tag{14}$$

$$X_{56} = N*C - \tfrac{1}{2}(D\sin\phi + E\cos\phi). \tag{15}$$

The rectangle defining the overlap coverage has area

$$\begin{aligned} A_o &= [(X_{34} - X_{35})/\sin\phi] * [(X_{35} - X_{56})/\cos\phi] \\ &= [D - N*C\cos\phi] * [E - N*C\sin\phi]. \end{aligned} \tag{16}$$

Finally, the spacing between adjacent paths is

$$C = (2\pi R_e\cos\theta)/233 \tag{17}$$

where R_e = 6370 km, the mean radius of the Earth.

Results

The areas of extended, missing, and overlap coverage, normalized to the area of a single scene (31,050 km^2), are shown as a function of row in Figure 6. Missing coverage is minimal at all

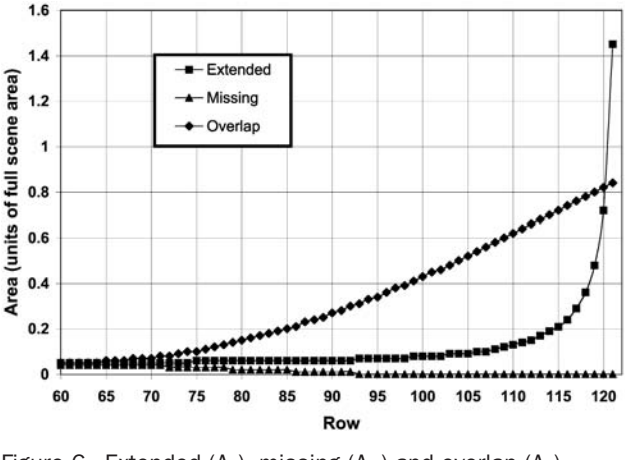

Figure 6. Extended (A_e), missing (A_m) and overlap (A_o) coverages versus WRS-2 rows 60 to 121.

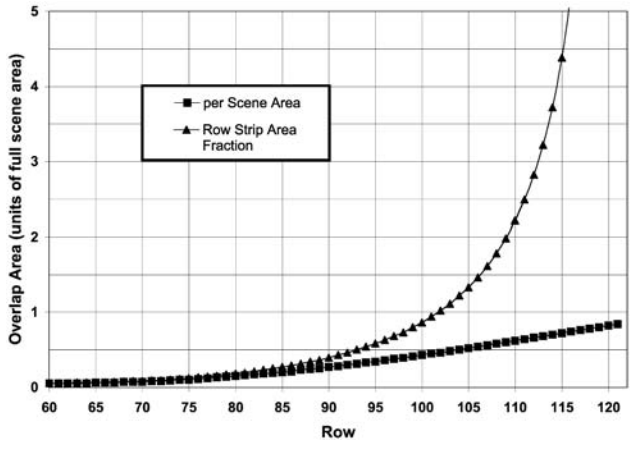

Figure 7. Overlap coverages A_o (per scene area) and A'_o (row strip area fraction) versus WRS-2 rows 60 to 121.

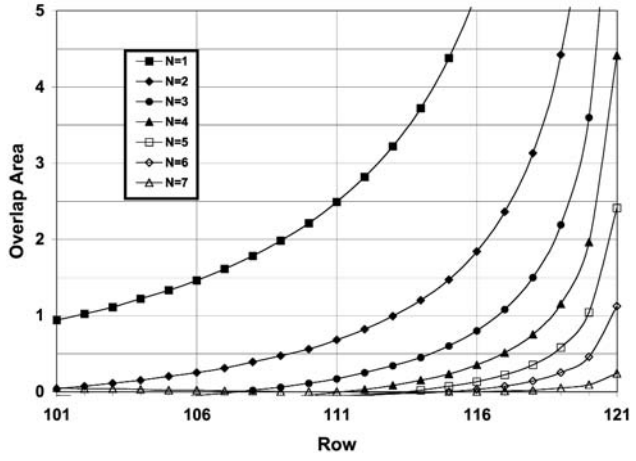

Figure 8. Overlap coverage A'_o (units of full scene area) versus WRS-2 rows 101 to 121 for different values of path spacing, N.

latitudes. This is expected because the sensor was designed to provide complete coverage at the equator. As latitude increases, the Earth's circumference along parallels of latitude decreases with no decrease in the 233 Landsat scenes distributed around that latitude. The reason A_m is not zero everywhere has to do with the manner in which it is defined in this paper. As row number increases, the bearing becomes larger. Both the increasing overlap and the narrowing row strip width combine to keep A_m low.

Extended coverage, A_e, increases nonlinearly with increasing row. This parameter is independent of adjacent scenes and increases as both the bearing of the scene increases and the width of the row strip decreases.

Finally, the overlap coverage, A_o, increases slowly at low latitudes, but grows nearly linearly through the mid- and high latitudes. The effect of increased bearing, which reduces overlap, slows the tendency of decreasing distance between scenes to increase overlap.

For large amounts of overlap, the row strip is oversampled. In principle, once overlap coverage exceeds half the scene area ($A_o > 0.5$) and A_m remains small, every other scene could be skipped and still cover the row strip. In practice, because the row strip narrows for these higher rows, some of the overlap falls outside the row strip, allowing path skipping to begin at even lower latitudes. Figure 7 illustrates this point by plotting overlap in units of scene area (A_o, as before) and as the fraction of row strip area. At row 102, the overlap area is just under half a scene, the fraction of row strip area is just over one, and recall that there is no missing coverage (A_m, from Figure 6). This indicates that most of the row strip is duplicated.

High-Latitude Coverage

The remainder of this analysis concentrates on the high latitudes because it is there that the increasing amount of overlap and extended coverage can lead to fewer scene acquisitions without sacrificing continuous coverage of the surface. Thus, the examination focuses on the effects of N greater than 1.

For this analysis, the coverages are expressed as fractions of the row strip area. The formulae for these parameters are

$$A'_e = 233\ A_e/(N * A_r), \tag{18}$$

$$A'_m = 233\ A_m/(N * A_r), \text{ and} \tag{19}$$

$$A'_o = 233\ A_o/(N * A_r), \tag{20}$$

where

$$A_r = 2\pi R_e \cos\theta * D \sin\phi \tag{21}$$

is the row strip area. The analysis is considered in two parts: overlap reduction by skipping paths, thus increasing the along-row distance between scenes, and making sure that the increased missing coverage caused by skipping paths is adequately compensated by the extended coverage.

Overlap

Figure 8 shows how overlap coverage (expressed as the fraction of row-strip area) is diminished as more paths are skipped. As an example, by skipping every other path (i.e., N = 2), overlap coverage would amount to 25 percent of the total row strip area at row 106. A similar amount of overlap could be achieved at row 119 by acquiring only every sixth scene.

Notches

Increasing N will decrease overlap but at the cost of increasing the missing coverage area, A_m. This missing area forms a sawtooth shape inside the row-strip boundary. Figure 9 shows

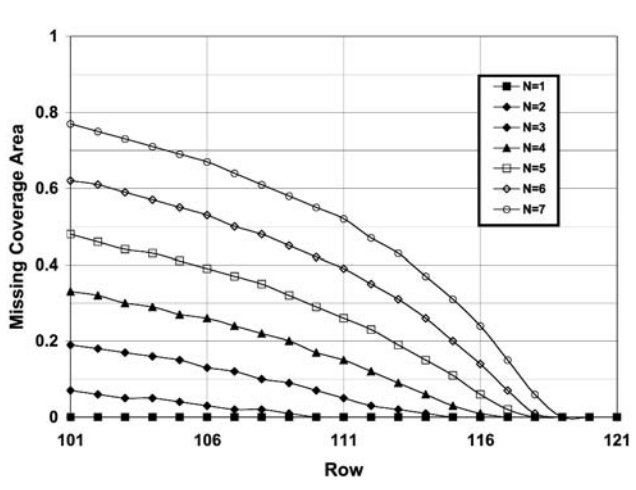

Figure 9. Missing coverage A'_m (units of full scene area) versus WRS-2 rows 101 to 121 for different values of path spacing, N.

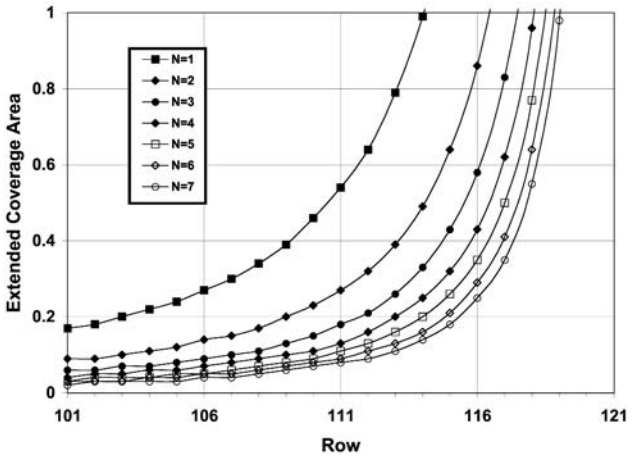

Figure 10. Extended coverage A'_e (units of full scene area) versus WRS-2 rows 101 to 121 for different values of path spacing, N.

how this area grows with increasing N. To use the example above, at row 106 the missing area is only 3 percent of the row strip area if every other scene is acquired. The effect diminishes with increasing row because the row strip width narrows. Beyond row 119, there is still no missing area even if only every seventh path is collected.

Extended coverage, A_e, from the neighboring row strips is also in the shape of a sawtooth boundary and must be relied on to fill the areas of missing coverage. Figure 10 shows how this area varies with row and value of N. A'_e increases with increasing row, first because groundtrack bearing increases and, at higher rows, because row-strip width decreases. As N increases, the number of scenes decreases, decreasing the fractional contribution of A'_e; however, this effect is almost compensated by the decreasing row strip area.

The triangular shapes of A_e and A_m are geometrically similar (c.f., Figure 3), sharing the same internal angle, but the arrangement of extended and missing coverages cannot be expected to line up perfectly. An excess of extended coverage will nearly always be required to ensure that missing coverage areas are eliminated.

Application

Two demonstrations are given of how these calculations can be used to construct an efficient collection strategy for Landsat imagery in the high latitudes. In the first demonstration case (Case 1), a conservative requirement of 25 percent overlap is stipulated while, in the second case (Case 2), 10 percent overlap is required. Table 1 shows the values of the maximum value of N for each row that produces at least 25 percent overlap or at least 10 percent overlap. But this is only part of the requirement. There must be sufficient extended coverage to compensate for the missing coverage. This is checked by finding the minimum A'_e from the previous row or next row. In the 25 percent overlap case, the minimum A'_e is always many times the value of A'_m for every row, ensuring that extended coverage will do an adequate job of filling any holes of A'_m. However, in the 10 percent overlap case, there are a few rows, particularly row 104, where the minimum A'_e is only slightly larger than the corresponding A'_m. With this strategy, some small holes in coverage are likely.

Figure 11 shows the spatial coverage that results from the parameters chosen in Table 1 for Case 2 (10 percent overlap). Small gaps occur when the skipping parameter changes between adjacent rows. These gaps, seen in Figure 11 immediately north of rows 110, 114, and 116, are caused by the relative positions of the extended and missing coverage areas.

TABLE 1. TWO EXAMPLES OF SCENE SAMPLING STRATEGIES COVERING THE SOUTHERN HIGH LATITUDES (ROWS 101 TO 121). CASE 2 IS ILLUSTRATED GRAPHICALLY IN FIGURE 11

	Case 1			Case 2		
Row	Maximum N ($A'_o > .25$)	Minimum A'_e in Adjacent Row	A'_m	Maximum N ($A'_o > .10$)	Minimum A'_e in Adjacent Row	A'_m
101	1	0.16	0	1	0.16	0
102	1	0.17	0	1	0.17	0
103	1	0.18	0	2	0.18	0.05
104	1	0.20	0	2	0.10	0.05
105	1	0.14	0	2	0.11	0.04
106	2	0.15	0.03	2	0.15	0.03
107	2	0.14	0.02	2	0.14	0.02
108	2	0.15	0.02	2	0.15	0.02
109	2	0.17	0.01	2	0.17	0.01
110	2	0.20	0	3	0.20	0.07
111	2	0.21	0	3	0.15	0.05
112	3	0.26	0.03	3	0.26	0.03
113	3	0.21	0.02	3	0.21	0.02
114	3	0.26	0.01	4	0.26	0.06
115	4	0.21	0.03	4	0.21	0.03
116	4	0.32	0.01	5	0.32	0.06
117	5	0.43	0	5	0.43	0.02
118	5	0.50	0	6	0.50	0.01
119	6	0.77	0	6	0.77	0
120	6	1.14	0	6	1.14	0
121	7	2.57	0	7	2.57	0

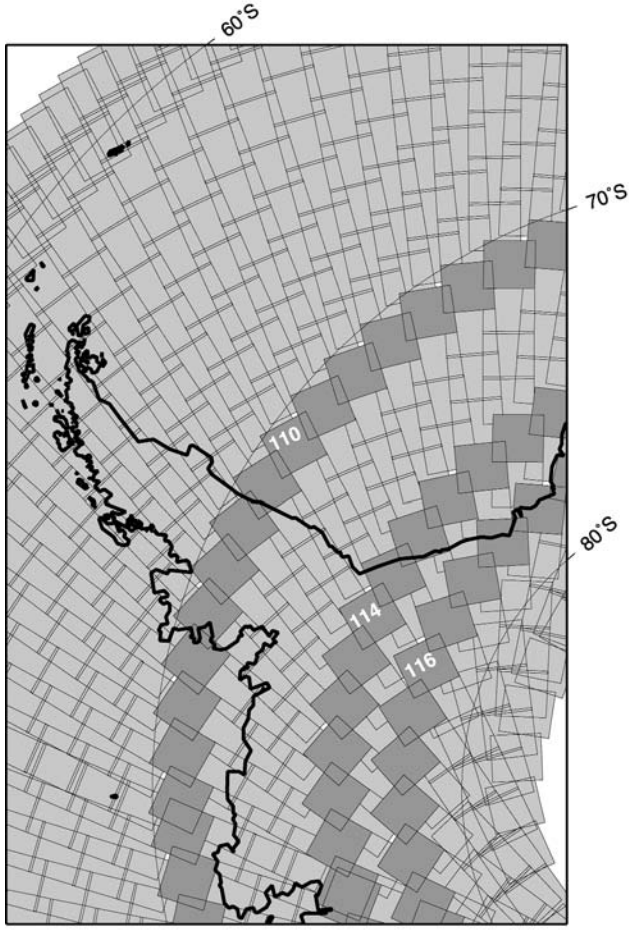

Case 2: $A_o' > .10$

Figure 11. Coverage plot of a portion of Antarctica for Case 2 (A_o' greater than 10 percent) discussed in text and shown in Table 1. Rows range from 101 (upper left) to 122 (lower right). Very small gaps are seen immediately north of the more darkly shaded rows 110, 114, and 116, when the path-skipping parameter is changed (see Table 1).

Case 1, with lower values of missing coverage and larger values of extended coverage, created no gaps.

The advantages of such sampling strategies are realized in the fewer images required to attain full coverage. For the case of Antarctica, coverage begins at row 103 and extends to row 122. There are 4660 scenes (233 by 20) contained within this area. By sampling according to Case 1 (25 percent overlap), full coverage is attained with only 1993 images. This is 43 percent of the total number of scenes possible. For Case 2, the total scenes required is only 1528, 33 percent of the total possible. This latter case does include some gaps, but much of the lower numbered rows (where paths are less frequently skipped) are located in the oceans beyond Antarctica and would not need to be included. The cases presented here are illustrative of the magnitude of reduced image requirements possible in the high latitudes without sacrificing ground coverage.

Summary

Landsat orbits converge at high latitudes, increasing the frequency and redundancy of ground coverage. Increased data volume can be advantageous, but is acquired by expending limited satellite resources. Scene orientation and spacing change rapidly at high latitudes as does the local time of acquisition. Consideration of the extended, missing, and overlap coverage of scenes centered at the same latitude provides a means to plan complete ground coverage with efficient acquisition strategies. This approach can easily be extended to ground coverage for any swath imaging satellite.

Acknowledgments

This work was completed to assist in the high latitude coverage strategy of the Landsat 7 Long Term Acquisition Plan. Patricia Vornberger helped with the demonstration cases. Financial support was provided by the NASA Earth Science Enterprise.

Reference

Arvidson, T., J. Gasch, and S.N. Goward, 2001. Landsat 7's long-term acquisition plan—An innovative approach to building a global imagery archive, *Remote Sensing of Environment*, 78(1-2):13–26.

(Received 18 March 2002; accepted 05 November 2002; revised 30 January 2003)